Hindawi Publishing Corporation
Journal of Nanomaterials
Volume 2014, Article ID 780686, 9 pages
http://dx.doi.org/10.1155/2014/780686

Research Article

Sm:HAp Nanopowders Present Antibacterial Activity against *Enterococcus faecalis*

Carmen Steluta Ciobanu,[1] Cristina Liana Popa,[1,2] and Daniela Predoi[1]

[1] *National Institute of Materials Physics, P.O. Box MG 07, 76900 Bucharest, Romania*
[2] *Faculty of Physics, University of Bucharest, 405 Atomistilor, P.O. Box MG-1, 077125 Bucharest, Romania*

Correspondence should be addressed to Daniela Predoi; dpredoi@gmail.com

Received 22 January 2014; Accepted 24 February 2014; Published 17 April 2014

Academic Editor: Necdet Aslan

The synthesis of nanoparticles with inhibitory and bactericidal effects represents a great interest in development of new materials for biological applications. In this paper we present for the first time the synthesis of $Ca_{10-x}Sm_x(PO_4)_6(OH)_2$ nanoparticles at low temperature and primary tests concerning the adherence of *Enterococcus faecalis ATCC 29212* (gram-positive bacteria). All the XRD peaks were indexed in accordance with the hexagonal HAp in P63m space group. The EDAX spectrum and elemental mapping of O, P, Ca, and Sm demonstrate that all the elements were homogeneously distributed in $Ca_{10-x}Sm_x(PO_4)_6(OH)_2$ with $x_{Sm} = 0.03$. The peaks at 347.3 eV, 532.1 eV, and 133.8 eV in the XPS spectra can be attributed to the binding energy of Ca 2p, O 1s, and P 2p. The peak at 1084.4 eV observed in $Ca_{10-x}Sm_x(PO_4)_6(OH)_2$ was attributed to the Sm $3d_{5/2}$. Bacterial adhesion was reduced on $Ca_{10-x}Sm_x(PO_4)_6(OH)_2$ sample when compared to pure HAp ($x_{Sm} = 0$) and significant differences in bacterial adhesion on pure HAp ($x = 0$) and Sm:HAp ($x_{Sm} = 0.01$, $x_{Sm} = 0.03$, and $x_{Sm} = 0.1$) were observed. The bacterial adhesion decreased when the samarium concentrations increased. Finally, we demonstrate that the Sm:HAp nanopowder with $x_{Sm} > 0$ showed high antibacterial activity against *Enterococcus faecalis ATCC 29212*.

1. Introduction

In the past decades scientists worldwide have tried to find new solutions for improving treatments used for different bone related diseases and injuries. Their attention has been focused to the field of biomaterials in order to create and develop new and improved materials for tissue engineering [1–3]. Among these materials, hydroxyapatite (HAp) is one of the most commonly used for bone implants [4–9] or it is a drug release system [4, 10–15]. Moreover, it has been shown that it is also a good candidate for the role of adsorbent in column chromatography, in order to separate and purify nucleic acids and proteins [3, 16, 17]. It is possible to use hydroxyapatite for a large number of applications in the biomedical field due to its remarkable properties, such as biocompatibility, bioactivity, and osteoconductivity [4, 18–21]. In live tissue, HAp is the major mineral component of human bones and teeth [4, 22, 23]. Various factors, such as grain size, morphology, surface area, and microporosity [24–26], must be taken into account when developing the biomaterial. Therefore, in order to improve the properties of HAp (for its use in different bone tissue applications), researchers have developed various methods of obtaining new compounds based on HAp doped with different rare-earth (RE) ions [24, 27]. The choice for lanthanides as doping agents has been made due to their high bioactivity and their ability to substitute calcium ions in structured molecules [24, 28–30]. It has been reported that lanthanides have been previously used in the biomedical field as contrast agents for magnetic resonance imaging and as luminescent probes for biosensors used for various *in vivo* imaging applications [24, 28, 29, 31], due to their narrow emission bands and long emission lifetime [24, 32, 33]. Among the rare-earth elements, samarium (Sm) is a good candidate for different radiation therapies used for cancer treatments. For more than a decade, ^{153}Sm isotopes have been used for cancer radiation

treatments [4, 34, 35] which are now administered clinically to patients that have symptomatic bone metastases from different types of cancer, mostly prostatic and breast carcinoma, for pain alleviation [4, 34–37]. In addition, different new studies have used ^{153}Sm-hydroxyapatite particles as radiation synovectomy agent in the treatment of chronic synovitis [38–41], especially knee synovitis [38, 39]. Radiation synovectomy is a method used to alleviate the pain of patients suffering from swelling of rheumatoid arthritis [42]. Furthermore, another major problem encountered in the medical field is the inflammation of the synovial membrane caused by prosthetic joint infections (PJI) [43] which could also be treated by radiation synovectomy. The procedure involves an intra-articular injection of the beta-emitting radiopharmaceutical into the joint space. Once the radionucleide decays, the regenerating synovium starts to be irradiated [41]. Therefore, the ^{153}Sm-hydroxyapatite particles are better candidates for this type of treatment than other compounds based on Y-90 due to the shorter half-life of ^{153}Sm and the lower extra-articular leakage of ^{153}Sm-hydroxyapatite [39]. Furthermore, it has been shown that ^{153}Sm emits β rays with a small tissue penetration (0.8 mm), more that 99% of the ^{153}Sm being bound to the hydroxyapatite *in vivo* [44]. According to a clinical study made by Brazilian researchers after one year of treatment based on ^{153}Sm-hydroxyapatite on patients suffering from haemophilic arthropathy, it was established that this treatment is effective for several types of joints. They obtained good results for 75% of elbows, 87.5% of ankles, and 40% of knees [45].

The prior studies have focused on preparation and characterization of complexes of europium (III) metal ion with organic reagents [46]. On the other hand, previous studies concerning the antibacterial and antifungal activity of ligand and its metal complexes tested against gram-positive and gram-negative bacteria, yeast, and fungi show that the complexes are more potent antimicrobials than the parent ligand [47–49].

The studies on the preparation, physicochemical characterization, and biological properties of the samarium doped hydroxyapatite (Sm:HAp) powders are absent in the literature. In this paper we present for the first time a method to synthesize the nanocrystalline hydroxyapatite doped with samarium at low temperature. Physicochemical characterization and antimicrobial studies on the Sm:HAp nanopowder are also presented for the first time. The results obtained suggest that the new obtained material, ^{153}Sm-hydroxyapatite, could be a good candidate for treating the inflamed and damaged synovial membrane of the joint encountered in the case of prosthetic joint infections.

The $Ca_{10-x}Sm_x(PO_4)_6(OH)_2$ powders were synthesized by coprecipitation method at low temperature, mixing $Sm(NO_3)_3{\cdot}6H_2O$, $Ca(NO_3)_2{\cdot}4H_2O$, and $(NH_4)_2HPO_4$ in deionized water. The structure, morphology, and vibrational properties of the obtained samples were studied by X-ray diffraction (XRD), scanning electron microscopy (SEM), and Fourier transform infrared spectroscopy (FT-IR). In order to reveal the presence of the samarium in the Sm:HAp nanopowder with x_{Sm} = 0.01, 0.03, and 0.1, the X-ray photoelectron spectroscopy (XPS) results are also presented. In addition, the preliminary antibacterial activity of the $Ca_{10-x}Sm_x(PO_4)_6(OH)_2$ nanopowder with x_{Sm} = 0.01, 0.03, and 0.1 is reported.

2. Experimental Section

2.1. Sample Preparation. All the reagents used for the synthesis, including ammonium dihydrogen phosphate [$(NH_4)_2HPO_4$], calcium nitrate tetrahydrate [$Ca(NO_3)_2{\cdot}4H_2O$], and Samarium(III) nitrate hexahydrate $Sm(NO_3)_3{\cdot}6H_2O$ (Sigma-Aldrich), were purchased without further purification.

Nanocrystalline hydroxyapatite doped with Sm, $(Ca_{10-x}Sm_x(PO_4)_6(OH)_2$, with x_{Sm} = 0 to x_{Sm} = 0.1 was obtained by setting the atomic ratio of Sm/[Sm+Ca] from 0% to 10% and [Ca+Sm]/P as 1.67. The $Sm(NO_3)_3{\cdot}6H_2O$ and $Ca(NO_3)_2{\cdot}4H_2O$ were dissolved in deionised water to obtain 300 mL [Ca+Sm] containing solution. On the other hand, the $(NH_4)_2HPO_4$ was dissolved in deionised water to make 300 mL P-containing solution. The [Ca+Sm] containing solution was put into a Berzelius and stirred at 100°C for 30 minutes. Meanwhile, the pH of P-containing solution was adjusted to 10 with NH_3 and stirred continuously for 30 minutes. The P-containing solution was added drop by drop into the [Ca+Sm] containing solution and stirred for 2 h, the pH being constantly adjusted and kept at 10. After the reaction, the deposited mixtures were washed several times with deionised water. The resulting material (Sm:HAp) was dried at 100°C. The scheme of the present study is presented in Figure 1.

2.2. Sample Characterization. The X-ray diffraction measurements of $Ca_{10-x}Sm_x(PO_4)_6(OH)_2$ samples were recorded using a Bruker D8 Advance diffractometer, with nickel filtered Cu K_α (λ = 1.5418 Å) radiation and a high efficiency one-dimensional detector (Lynx Eye type) operated in integration mode. The diffraction patterns were collected in the 2θ range 15°–140°, with a step of 0.02° and 34 s measuring time per step.

The scanning electron microscopy (SEM) study was performed on a HITACHI S2600N-type microscope equipped with an energy dispersive X-ray attachment (EDAX/2001 device). Energy dispersive X-ray analysis, referred to as EDS or EDAX, was used to identify the elemental composition of materials.

The functional groups present in the prepared nanoparticles and thin films were identified by FTIR using a Spectrum BX spectrometer. In order to obtain the nanoparticles spectra, 1% of nanopowder was mixed and ground with 99% KBr. Tablets of 10 mm diameter were prepared by pressing the powder mixture at a load of 5 tons for 2 min. The spectrum was taken in the range of 500 to 4000 cm^{-1} with 4 cm^{-1} resolution.

X-ray photoelectron spectroscopy (XPS) studies were conducted using a VG ESCA 3 MK II XPS installation ($E_{k\alpha}$ = 1486.7 eV). The vacuum analysis chamber pressure was $P \sim 3 \times 10^{-8}$ torr. The XPS recorded spectrum involved an energy window w = 20 eV with the resolution R = 50 eV with 256

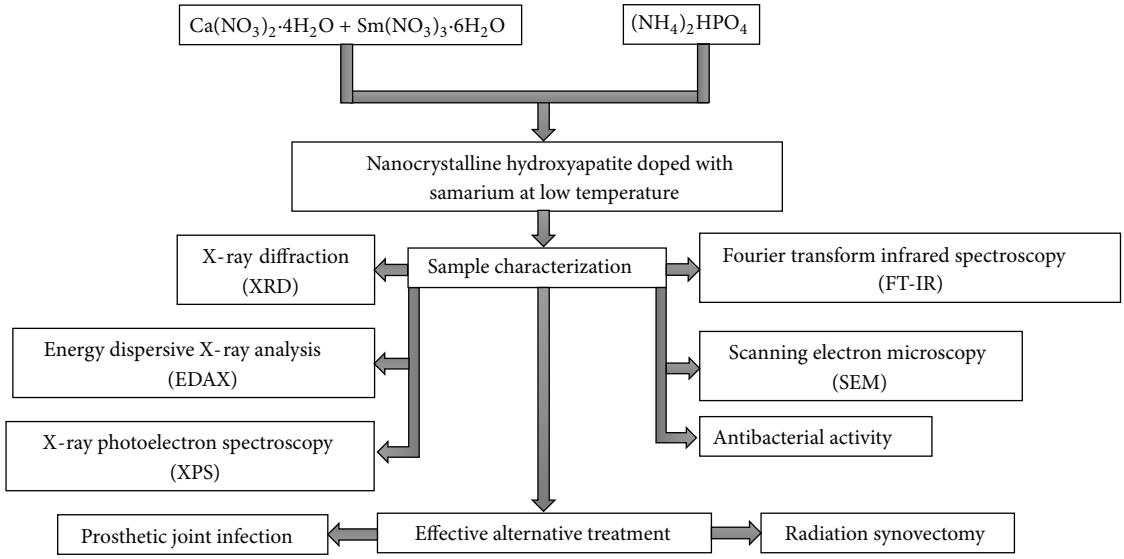

Figure 1: Schematic representation of preparation and evaluation of new antimicrobial Sm:HAp ceramics.

Table 1: Lattice parameters of Sm doped hydroxyapatite and crystallite sized.

Samples	a-axis (Å)	c-axis (Å)	Unit cell volume (Å)	Crystallite size D (nm)
$x_{Sm} = 0.01$	9.4195	6.8857	528.8875	18.14
$x_{Sm} = 0.03$	9.4299	6.8864	529.9895	17.53
$x_{Sm} = 0.1$	9.4398	6.8897	531.5923	12.67

recording channels. The XPS spectra were processed using Spectral Data Processor v 2.3 (SDP) software.

In order to test the *in vitro* antibacterial activity, the strains of bacteria used were *Enterococcus faecalis ATCC 29212*. The bacteria were grown overnight in Todd-Hewit broth supplemented with 1% yeast extract at 37°C, followed by centrifuging. The supernatants were discarded and pellets were resuspended in phosphate-buffered saline (PBS) followed by a second centrifuging and resuspension in PBS. The samples to be tested were placed in 50 mL sterilized tubs followed by the addition of 2 mL of the bacterial suspension. The tubes were incubated at 3°C for 4 h. At the end of the incubation period, the samples were gently rinsed three times with PBS. The nonadherent bacteria were eliminated. After washing, the samples were then put into a new tube containing 5 mL PBS and vigorously vortexed for 30 s to remove the adhering microorganisms. The viable organisms in the buffer were quantified by plating serial dilutions on yeast extract agar plates. Yeast extract agar plates were incubated for 24 h at 3°C and the colony forming units were counted visually.

3. Results and Discussions

In Figure 2 the XRD patterns of the synthesized $Ca_{10-x}Sm_x(PO_4)_6(OH)_2$ nanopowders with $x_{Sm} = 0.01$, 0.03, and 0.1 are shown. Good pattern fit of the synthetized Sm:HAp structures was determined using the Rietveld method implemented in the software package Materials Analysis Using

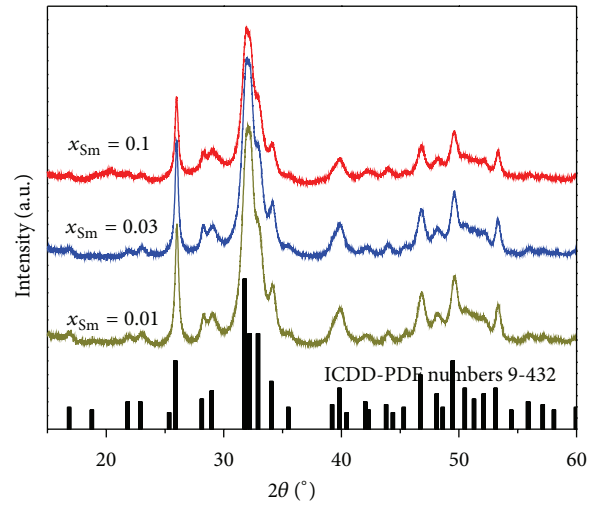

Figure 2: XRD patterns of $Ca_{10-x}Sm_x(PO_4)_6(OH)_2$ nanopowders with $0.01 \leq x_{Sm} \leq 0.1$.

Diffraction (MAUD) [50] by applying the Popa approach for the anisotropic microstructure analysis [51] implemented in the MAUD as "Popa rules."

The XRD patterns of the Sm:HAp nanopowders with x_{Sm} = 0.01, 0.03, and 0.1 appeared to be identical, regardless of the Sm content in the samples. Sm doped hydroxyapatite exerted no effect on the phase composition of pure HAp.

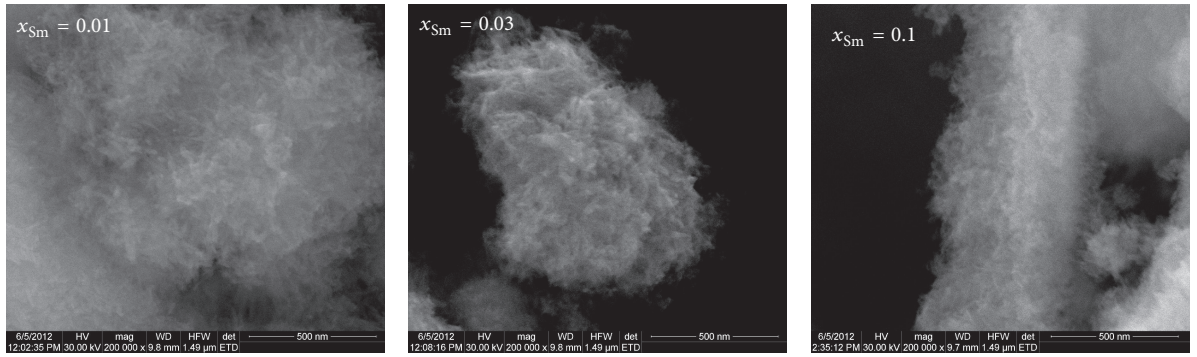

Figure 3: SEM images of samarium doped hydroxyapatite (Sm:HAp) powders with $x_{Sm} = 0.01$, $x_{Sm} = 0.03$, and $x_{Sm} = 0.1$.

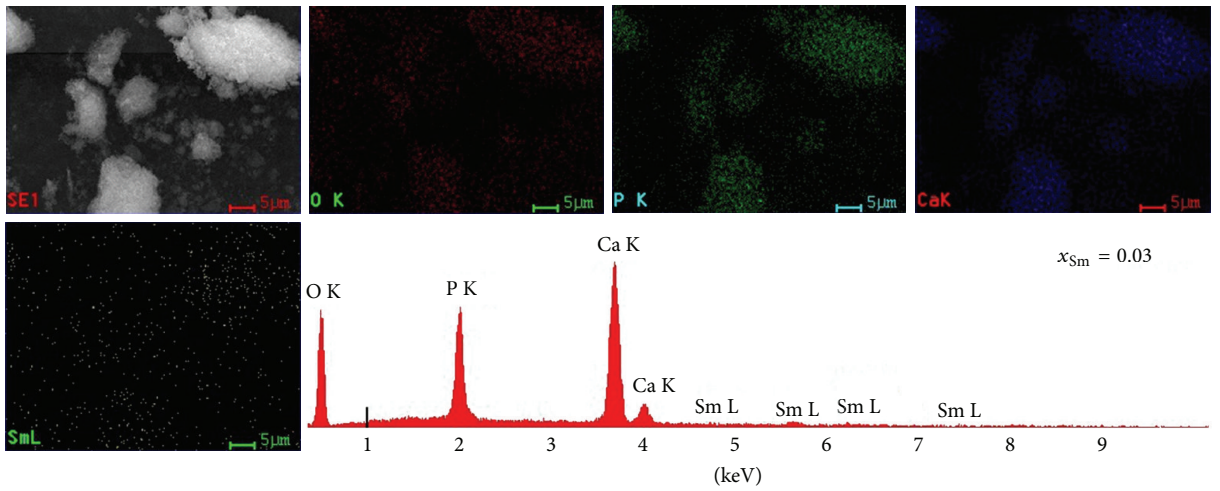

Figure 4: EDX spectrum and element maps of oxygen, phosphorus, calcium, and samarium (for the powders with $x_{Sm} = 0.03$).

No secondary phases than those associated with HAp were detected. All the XRD peaks were indexed in accordance with the hexagonal HAp in P_{63m} space group (JCPDS card number 9-432). On the other hand, no change took place in the symmetry of the HAp crystallographic unit cell.

In the XRD spectra of the Sm:HAp powders, the diffraction peak intensities were reduced and the peak shapes were broadened when the Sm concentration increased. The broadened peaks when Sm concentration increased in the Sm:HAp samples are attributed to the small grain size. However, small variations of lattice constants and crystallite size were observed when the samarium content increases as it can be seen in Table 1.

Typical particle morphology of the Sm:HAp (x_{Sm} = 0.01, x_{Sm} = 0.03 and x_{Sm} = 0.1.) samples are shown in Figure 3. The surface morphology investigated by scanning electron microscopy reveals that the particles have a small, long morphology, coexisting with agglomerates. The results suggest that the doping of Sm has little influence on the morphology of Sm:HAp samples.

In order to investigate the uniformity of the element distribution in Sm:HAp samples, the EDX mapping technique was used. Figure 4 shows the EDAX spectrum and elemental mapping of O, P, Ca, and Sm and demonstrates that all the elements were homogeneously distributed in $Ca_{10-x}Sm_x(PO_4)_6(OH)_2$ with $x_{Sm} = 0.03$. On the other hand, the purity of the synthetized powders was also demonstrated. Similar results regarding the homogenous distribution of O, P, Ca, and Sm in the Sm:HAp samples were obtained for all the analysed samples.

FT-IR spectroscopy was performed in order to investigate the functional groups present in the nanohydroxyapatite, $Ca_{10-x}Sm_x(PO_4)_6(OH)_2$ (x_{Sm} = 0.01, x_{Sm} = 0.03, and x_{Sm} = 0.1) samples. In Figure 5 the FT-IR spectra of samarium doped hydroxyapatite with various concentration are presented.

In the FT-IR spectra, the presence of $[OH]^-$ vibration peak at 632 cm^{-1} could be observed for all the samples [52]. This band arises from stretching vibrational mode of $[OH]^-$. According to Markovic et al. [53], the sharpness of bands, especially sharpness of the 632 cm^{-1}, 603 cm^{-1}, and

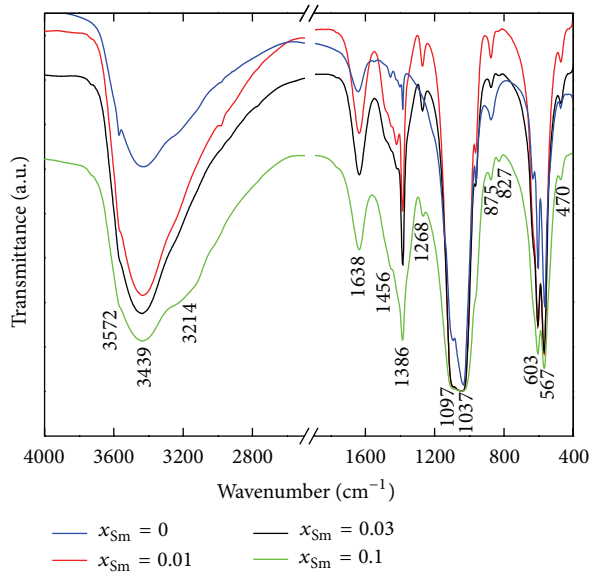

FIGURE 5: FT-IR spectra of samarium doped hydroxyapatite (Sm:HAp) with $x_{Sm} = 0$, $x_{Sm} = 0.01$, $x_{Sm} = 0.03$, and $x_{Sm} = 0.1$.

567 cm^{-1} bands, indicates a well-crystallized HAp. The band at 470 cm^{-1} is assigned to the ν_2 $[PO_4]^{3-}$ [54]. The vibration peaks in the regions 1600–1700 cm^{-1} and 3200–3600 cm^{-1} correspond to H–O–H bands of lattice water. The characteristic bands for carbonate are presented in the spectral regions 1400–1600 cm^{-1} (ν_3: asymmetric stretch vibration) and 873–880 cm^{-1} (ν_2: out-of-plane bend vibration). In addition, a weak band for the stretch vibration of structurally bound OH may be present in Sm:HAp samples near 3572 cm^{-1}. Generally, it is difficult to distinguish between HPO_4^{2-} and CO_3^{2-} groups due to the overlapping of the characteristic peaks around 870 cm^{-1} [55, 56].

The bands at around 1097 cm^{-1} and about 1037 cm^{-1} can be attributed to the ν_3 $[PO_4]^{3-}$, while the band at 962 arises from ν_1 $[PO_4]^{3-}$. The 603 cm^{-1} and 567 cm^{-1} bands appear from ν_4 $[PO_4]^{3-}$ [57, 58]. In the FT-IR spectrum (Figure 5) the bands corresponding to the ν_3 vibration of C–O were observed at 1456 cm^{-1}, characteristic of the carbonate group [59, 60].

Also, in Figure 5 we observed that the contribution of the area that corresponds to the phosphate bands decreases when the samarium concentration in the samples increases. The bands at 632 and 962 cm^{-1} progressively disappear with the increase of samarium concentration. When $x_{Sm} = 0.1$ these bands are almost absent.

Furthermore, in agreement with the results already reported in the literature, it can be observed that the use of samarium as doping agent does not induce the appearance of other peaks [61–63].

The XPS analysis has been used to obtain the qualitative determination of the surface components and composition of the samples. Figure 6 shows the survey of XPS narrow scan spectra of the as-prepared $Ca_{10-x}Sm_x(PO_4)_6(OH)_2$ with $x_{Sm} = 0.01$ (a), $x_{Sm} = 0.03$ (b), and $x_{Sm} = 0.1$ (c) nanopowder samples. Concerning the binding energies in the pure HAp, the peaks at 347.3 eV, 532.1 eV and 133.8 eV can be attributed to the binding energy of Ca 2p, O 1s and P 2p, confirming the presence of apatite groups [64–66]. The peak at 1084,4 eV observed in $Ca_{10-x}Sm_x(PO_4)_6(OH)_2$ was attributed to the Sm $3d_{5/2}$, consistent with the normal oxidation state of Sm^{3+}, because the binding energy of core level for Sm_2O_3 is generally observed at 1083.2 eV [65].

The peaks associated to Ca, P, and O states presented in Figure 6 were the same in the Sm:HAp samples with different Sm^{3+} concentrations ($x_{Sm} = 0.01$ (a), $x_{Sm} = 0.03$ (b), and $x_{Sm} = 0.1$ (c)). This showed that the increasing of the concentration of Sm did not change the binding energy assigned to Ca 2p, O 1s, and P 2p presented in Sm:HAp samples. For XPS analysis, the binding energies were calibrated with reference C 1s at 285 eV. By combination of XRD results, it can be concluded that these signals can be assigned to Sm:HAp nanopowder. XPS results provided the additional evidence for the successful doping with Sm^{3+} in Sm:HAp.

In agreement with previous studies [52, 57, 67], the luminescence, magnetic, and nuclear properties of the ceramics can be improved by doping them with lanthanides. According to [68], the biocompatibility and valuable biological properties of samarium were proved by their use in drugs to regulate blood clotting present during the process of wound healing. Knowing that lanthanides (III) have an interesting biological role but not well known, preliminary antimicrobial tests were performed on samples of hydroxyapatite doped with samarium.

Figure 7 shows the results of viable bacteria adhering to the 5, 15, 25, and 50 μg/mL of $Ca_{10-x}Sm_x(PO_4)_6(OH)_2$ ($x_{Sm} = 0.01$, $x_{Sm} = 0.03$, and $x_{Sm} = 0.1$) when exposed to *Enterococcus faecalis ATCC 29212*. Bacterial adhesion was reduced on $Ca_{10-x}Sm_x(PO_4)_6(OH)_2$ sample when compared to pure HAp ($x_{Sm} = 0$) and significant differences in bacterial adhesion on pure HAp ($x = 0$) and Sm:HAp ($x_{Sm} = 0.01$, $x_{Sm} = 0.03$, and $x_{Sm} = 0.1$) were observed. We observed that the bacterial adhesion decreased when the samarium concentrations increased.

In this preliminary antimicrobial studies we observed that the Sm:HAp nanopowders have significantly lower adhesion of *Enterococcus faecalis ATCC 29212*, suggesting that the Sm:HAp nanopowders are antibacterial. In the future, the effect of samarium doped hydroxyapatite on other bacterial strains will be evaluated and these strains will be selected depending on the field of applications. The influence of the size of Sm:HAp nanoparticles on bacterial strains will be also studied.

The recent studies [69, 70] suggest that risk of infections in actual treatment of prosthetic infections is a major problem. In the patient treatment with hip or knee prosthetic infections it is noteworthy that infections with gram-negative bacilli or a fungus are contraindications. In this context, to optimize patient treatment with prosthetic infections the creation of new materials with antimicrobial properties is very important [71, 72]. In conclusion, it can be said that

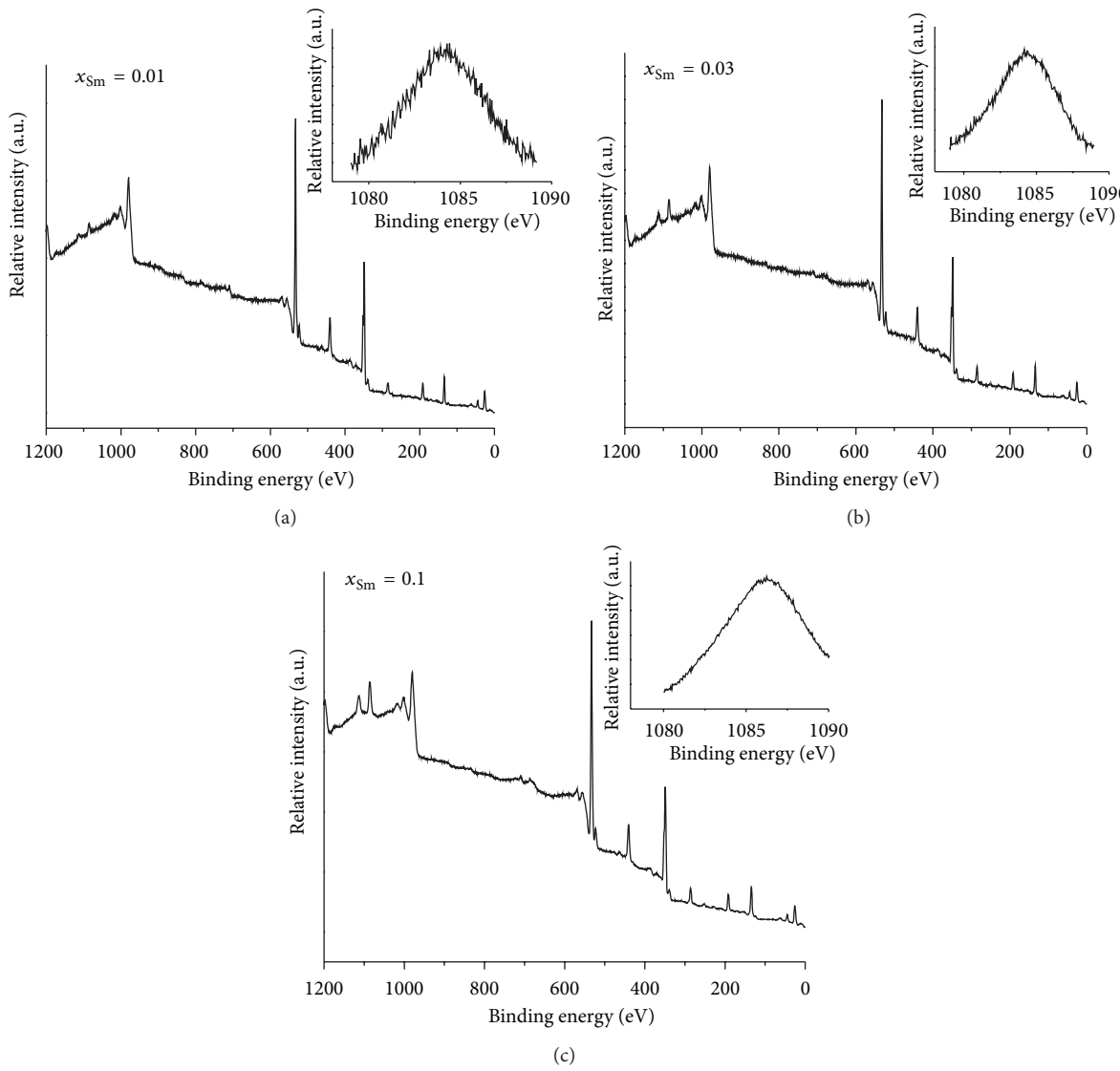

FIGURE 6: XPS general spectrum of $Ca_{10-x}Sm_x(PO_4)_6(OH)_2$ with x_{Sm} = 0.01 (a), x_{Sm} = 0.03 (b), and x_{Sm} = 0.1 (c) powders. XPS narrow scan spectra of Sm element are presented for all the samples.

the new bioceramic Sm:HAp with antimicrobial properties may be a candidate with a good outcome in prosthetic joint infection and bone-targeting drug delivery system.

4. Conclusions

In this short work, the emphasis was placed on the synthesis at low temperature by a simple method of pure Sm:HAp nanopowder with efficient antimicrobial activity.

The XRD studies have shown that the characteristic peaks of Sm:HAp nanopowders appeared to be identical regardless of the Sm content in the samples. All the XRD peaks were indexed in accordance with the hexagonal HAp in P_{63m} space group (JCPDS card number 9-432) and no other secondary phases were detected. The functional groups present in nanohydroxyapatite samples, $Ca_{10-x}Sm_x(PO_4)_6(OH)_2$ (x_{Sm} = 0.01, x_{Sm} = 0.03, and x_{Sm} = 0.1), were investigated by FT-IR spectroscopy. It has been observed that the use of samarium as doping agent does not induce the appearance of other peaks. FTIR spectra of the Sm:HAp samples show only the absorption bands characteristic to hydroxyapatite. A small long morphology was remarked for all the Sm:HAp nanopowder samples by SEM. The doping of Sm has little influence on the morphology of Sm:HAp samples. The presence and uniform distribution of samarium in the nanopowder samples were confirmed by elemental maps. The EDX spectrum of Sm:HAp confirms the presence of calcium (Ca), phosphorus (P), oxygen (O), and samarium (Sm) in all the synthetized samples. The successful doping of Sm^{3+} in Sm:HAp was also emphasized by XPS results.

The inhibition of *Enterococcus faecalis ATCC 29212* bacteria increased when the samarium concentrations in

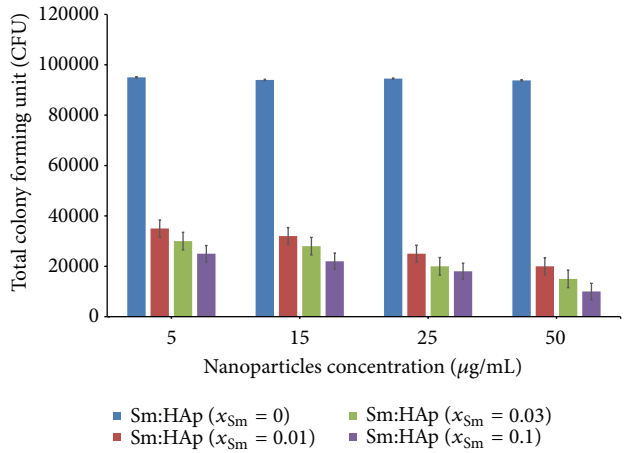

FIGURE 7: Adherence of *Enterococcus faecalis ATCC 29212* on different concentrations of $Ca_{10-x}Sm_x(PO_4)_6(OH)_2$ (x_{Sm} = 0.01, x_{Sm} = 0.03, and x_{Sm} = 0.1) nanopowders compared to pure HAp (x_{Sm} = 0) nanopowders.

$Ca_{10-x}Sm_x(PO_4)_6(OH)_2$ increased from x_{Sm} = 0.01 to x_{Sm} = 0.1. Our studies have shown that the $Ca_{10-x}Sm_x(PO_4)_6(OH)_2$ (x_{Sm} = 0.01, x_{Sm} = 0.03 and x_{Sm} = 0.1) exhibited greater antimicrobial activity compared to the pure HAp (x_{Sm} = 0). This will be significant for further antimicrobial studies of $Ca_{10-x}Sm_x(PO_4)_6(OH)_2$ on various gram-positive and gram-negative bacteria as well as fungi.

In conclusion, this study on new bioceramic Sm:HAp with antimicrobial properties may present a solution in bone-targeting drug delivery system and prosthetic joint infection. On the other hand, Sm:HAp bioceramics can be used as antimicrobial coatings in various applications.

Conflict of Interests

The authors declare that there is no conflict of interests regarding the publication of this paper.

Acknowledgments

The financial and encouraging support provided by the Ministry of Education of Romania under the Project IFA-CEA, no. C2-06, is acknowledged. The authors are grateful to Dr. Florica Frumosu, for XPS measurements. The authors also wish to thank Dr. Alina Mihaela Prodan for assistance with antibacterial assays.

References

[1] J. Hao, Y. Liu, S. Zhou, Z. Li, and X. Deng, "Investigation of nanocomposites based on semi-interpenetrating network of [L-poly (ε-caprolactone)]/[net-poly (ε-caprolactone)] and hydroxyapatite nanocrystals," *Biomaterials*, vol. 24, no. 9, pp. 1531–1539, 2003.

[2] C. R. Safinya and L. Addadi, "Biomaterials," *Current Opinion in Solid State and Materials Science*, vol. 2, no. 3, pp. 325–329, 1997.

[3] A. Groza, "Review of the processes identified during the polymerization of organic and organosilicon liquid films in atmospheric pressure air corona discharges," *Romanian Reports in Physics*, vol. 64, pp. 1227–1242, 2012.

[4] Y. J. Han, S. C. J. Loo, N. T. Phung, F. Boey, and J. Ma, "Controlled size and morphology of EDTMP-doped hydroxyapatite nanoparticles as model for ^{153}Samarium-EDTMP doping," *Journal of Materials Science: Materials in Medicine*, vol. 19, no. 9, pp. 2993–3003, 2008.

[5] D. A. Wahl and J. T. Czernuszka, "Collagen-hydroxyapatite composites for hard tissue repair," *European Cells and Materials*, vol. 11, pp. 43–56, 2006.

[6] J. Dumbleton and M. T. Manley, "Hydroxyapatite-coated prostheses in total hip and knee arthroplasty," *Journal of Bone and Joint Surgery A*, vol. 86, no. 11, pp. 2526–2540, 2004.

[7] P. Budrugeac, V. Trandafir, and M. G. Albu, "The effect of the hydration degree on the hydrothermal and thermo-oxidative stability of some collageneous matrices," *Journal of Thermal Analysis and Calorimetry*, vol. 72, no. 2, pp. 581–585, 2003.

[8] M. V. Ghica, M. G. Albu, M. Leca, L. Popa, and S. T. Moisescu, "Design and optimization of some collagen-minocycline based hydrogels potentially applicable for the treatment of cutaneous wound infections," *Pharmazie*, vol. 66, no. 11, pp. 853–861, 2011.

[9] J. S. Grimes, T. J. Bocklage, and J. D. Pitcher, "Collagen and biphasic calcium phosphate bone graft in large osseous defects," *Orthopedics*, vol. 29, no. 2, pp. 145–148, 2006.

[10] W. Paul and C. P. Sharma, "Ceramic drug delivery: a perspective," *Journal of Biomaterials Applications*, vol. 17, no. 4, pp. 253–264, 2003.

[11] T. Matsumoto, M. Okazaki, M. Inoue et al., "Hydroxyapatite particles as a controlled release carrier of protein," *Biomaterials*, vol. 25, no. 17, pp. 3807–3812, 2004.

[12] A. Uchida, Y. Shinto, N. Araki, and K. Ono, "Slow release of anticancer drugs from porous calcium hydroxyapatite ceramic," *Journal of Orthopaedic Research*, vol. 10, no. 3, pp. 440–445, 1992.

[13] Y. Shinto, A. Uchida, F. Korkusuz, N. Araki, and K. Ono, "Calcium hydroxyapatite ceramic used as a delivery system for antibiotics," *Journal of Bone and Joint Surgery B*, vol. 74, no. 4, pp. 600–604, 1992.

[14] M. Itokazu, W. Yang, T. Aoki, A. Ohara, and N. Kato, "Synthesis of antibiotic-loaded interporous hydroxyapatite blocks by vacuum method and in vitro drug release testing," *Biomaterials*, vol. 19, no. 7–9, pp. 817–819, 1998.

[15] A. Barroug and M. J. Glimcher, "Hydroxyapatite crystals as a local delivery system for cisplatin: adsorption and release of cisplatin in vitro," *Journal of Orthopaedic Research*, vol. 20, no. 2, pp. 274–280, 2002.

[16] M. J. Gorbunoff, "Protein chromatography on hydroxyapatite columns," *Methods in Enzymology*, vol. 117, pp. 370–380, 1985.

[17] S. Doonan, "Chromatography on hydroxyapatite," *Methods in Molecular Biology*, vol. 244, pp. 191–194, 2004.

[18] M. Vallet-Regí, "Ceramics for medical applications," *Journal of the Chemical Society*, vol. 2, pp. 97–108, 2001.

[19] L. Hermansson, L. Kraft, and H. Engqvist, "Chemically bonded ceramics as biomaterials," *Key Engineering Materials*, vol. 247, pp. 437–442, 2003.

[20] T. Kokubo, H. Kim, and M. Kawashita, "Novel bioactive materials with different mechanical properties," *Biomaterials*, vol. 24, no. 13, pp. 2161–2175, 2003.

[21] M. Shirkhanzadeh, "Microneedles coated with porous calcium phosphate ceramics: effective vehicles for transdermal delivery of solid trehalose," *Journal of Materials Science: Materials in Medicine*, vol. 16, no. 1, pp. 37–45, 2005.

[22] K. Shigeru, T. Oku, and S. Takagi, "Hydraulic property of hydroxyapatite thermal decomposition product and its application as biomaterial," *Journal of the Ceramic Society of Japan. International Edition*, vol. 97, pp. 96–101, 1989.

[23] M. Jarcho, C. H. Bolen, M. B. Thomas, J. Bobick, J. F. Kay, and R. H. Doremus, "Hydroxylapatite synthesis and characterization in dense polycrystalline form," *Journal of Materials Science*, vol. 11, no. 11, pp. 2027–2035, 1976.

[24] J. Coelho, N. S. Hussain, P. S. Gomes et al., "Development and characterization of lanthanides doped hydroxyapatite composites for bone tissue application," in *Current Trends on Glass and Ceramic Materials*, pp. 87–115, Scopus, 2013.

[25] D. Veljović, R. Jančić-Hajneman, I. Balać et al., "The effect of the shape and size of the pores on the mechanical properties of porous HAP-based bioceramics," *Ceramics International*, vol. 37, no. 2, pp. 471–479, 2011.

[26] T. Kokubo, *Bioceramics and Their Clinical Applications*, Woodhead Publishing Limited and CRC Press, 2008.

[27] A. Aissa, M. Debbabi, M. Gruselle et al., "Sorption of tartrate ions to lanthanum (III)-modified calcium fluor- and hydroxyapatite," *Journal of Colloid and Interface Science*, vol. 330, no. 1, pp. 20–28, 2009.

[28] S. P. Fricker, "The therapeutic application of lanthanides," *Chemical Society Reviews*, vol. 35, no. 6, pp. 524–533, 2006.

[29] K. H. Thompson and C. Orvig, "Lanthanide compounds for therapeutic and diagnostic applications," *Chemical Society Reviews*, vol. 35, no. 6, p. 499, 2006.

[30] T. Matsuda, C. Yamanaka, and M. Ikeya, "ESR study of Gd^{3+} and Mn^{2+} ions sorbed on hydroxyapatite," *Applied Radiation and Isotopes*, vol. 62, no. 2, pp. 353–357, 2005.

[31] Y. Fan, S. Huang, J. Jiang et al., "Luminescent, mesoporous, and bioactive europium-doped calcium silicate (MCS: Eu^{3+}) as a drug carrier," *Journal of Colloid and Interface Science*, vol. 357, no. 2, pp. 280–285, 2011.

[32] M. Neumeier, L. A. Hails, S. A. Davis, S. Mann, and M. Epple, "Synthesis of fluorescent core-shell hydroxyapatite nanoparticles," *Journal of Materials Chemistry*, vol. 21, no. 4, pp. 1250–1254, 2011.

[33] I. A. Appavoo and Y. Zhang, "Upconverting fluorescent nanoparticles for biological applications," in *Emerging Nanotechnologies for Manufacturing*, A. Waqar and J. J. Mark, Eds., pp. 159–175, William Andrew, Boston, Mass, USA, 2010.

[34] J. H. Turner, P. G. Claringbold, E. L. Hetherington, P. Sorby, and A. A. Martindale, "A phase I study of samarium-153 ethylenediaminetetramethylene phosphonate therapy for disseminated skeletal metastases," *Journal of Clinical Oncology*, vol. 7, no. 12, pp. 1926–1931, 1989.

[35] J. H. Turner and P. G. Claringbold, "A phase II study of treatment of painful multifocal skeletal metastases with single and repeated dose samarium-153 ethylenediaminetetramethylene phosphonate," *European Journal of Cancer*, vol. 27, no. 9, pp. 1084–1086, 1991.

[36] J. F. Eary, C. Collins, M. Stabin et al., "Samarium-153-EDTMP biodistribution and dosimetry estimation," *Journal of Nuclear Medicine*, vol. 34, no. 7, pp. 1031–1036, 1993.

[37] D. A. Podoloff, L. P. Kasi, E. E. Kim, F. Fossella, and V. A. Bhadkamar, "Evaluation of Sm-153-EDTMP as a bone imaging agent during a therapeutical trial," *Journal of Nuclear Medicine*, vol. 32, p. A918, 1991.

[38] M. F. dos Santos, R. N. V. Furtado, M. S. Konai, M. L. V. Castiglioni, R. R. Marchetti, and J. Natour, "Effectiveness of radiation synovectomy with samarium-153 particulate hydroxyapatite in rheumatoid arthritis patients with knee synovitis: a controlled randomized double-blind trial," *Clinics*, vol. 64, no. 12, pp. 1187–1193, 2009.

[39] E. K. O'Duffy, F. J. Oliver, S. J. Chatters et al., "Chromosomal analysis of peripheral lymphocytes of patients before and after radiation synovectomy with samarium-153 particulate hydroxyapatite," *Rheumatology*, vol. 38, no. 4, pp. 316–320, 1999.

[40] E. K. O'Duffy, G. P. R. Clunie, D. Lui, J. C. W. Edwards, and P. J. Ell, "Double blind glucocorticoid controlled trial of samarium-153 particulate hydroxyapatite radiation synovectomy for chronic knee synovitis," *Annals of the Rheumatic Diseases*, vol. 58, no. 9, pp. 554–558, 1999.

[41] P. Pusuwan, P. Asavatanabodee, and P. Chaudakshetrin, "Radiation synovectomy with Samarium-153 particulate hydroxyapatite: a preliminary report," in *Proceedings of the International Atomic Energy Agency-Publications-Iaea SR, 209, SR-209/52 Therapeutic Applications of Radiopharmaceuticals International Seminar, Therapeutic Applications of Radiopharmaceuticals*, International Atomic Energy, Agency, 1999.

[42] G. Clunie, D. Lui, I. Cullum, J. C. W. Edwards, and P. J. Ell, "Samarium-153-particulate hydroxyapatite radiation synovectomy: biodistribution data for chronic knee synovitis," *Journal of Nuclear Medicine*, vol. 36, no. 1, pp. 51–57, 1995.

[43] International Consensus on Periprosthetic Joint Infection, The Musculoskeletal Infection Society, http://www.msis-na.org/international-consensus/.

[44] M. Chinol, S. Vallabhajosula, S. J. Goldsmith et al., "Chemistry and biological behavior of samarium-153 and rhenium-186-labeled hydroxyapatite particles: potential radiopharmaceuticals for radiation synovectomy," *Journal of Nuclear Medicine*, vol. 34, no. 9, pp. 1536–1542, 1993.

[45] J. U. Calegaro, J. C. de Paula, J. S. C. de Almeida, and L. A. Casulari, "Clinical evaluation after 1 year of 153-samarium hydroxyapatite synovectomy in patients with haemophilic arthropathy," *Haemophilia*, vol. 15, no. 1, pp. 240–246, 2009.

[46] Y. Wang, R. Hu, D. Jiang, P. Zhang, Q. Lin, and Y. Wang, "Synthesis, crystal structure, interaction with BSA and antibacterial activity of La(III) and Sm(III) complexes with enrofloxacin," *Journal of Fluorescence*, vol. 21, no. 2, pp. 813–823, 2011.

[47] Y. F. Zhao, H. B. Chu, F. Bai et al., "Synthesis, crystal structure, luminescent property and antibacterial activity of lanthanide ternary complexes with 2, 4, 6-tri(2-pyridyl)-s-triazine," *Journal of Organometallic Chemistry*, vol. 716, pp. 167–174, 2012.

[48] A. M. Ajlouni, Z. A. Taha, W. Al Momani, A. K. Hijazi, and M. Ebqa'ai, "Synthesis, characterization, biological activities, and luminescent properties of lanthanide complexes with N,N′-bis(2-hydroxy-1-naphthylidene)-1,6-hexadiimine," *Inorganica Chimica Acta*, vol. 388, pp. 120–126, 2012.

[49] K. Mohanan, B. S. Kumari, and G. Rijulal, "Microwave assisted synthesis, spectroscopic, thermal, and antifungal studies of some lanthanide(III) complexes with a heterocyclic bishydrazone," *Journal of Rare Earths*, vol. 26, no. 1, pp. 16–21, 2008.

[50] L. Lutterotti, "Total pattern fitting for the combined size-strain-stress-texture determination in thin film diffraction," *Nuclear Instruments and Methods in Physics Research B: Beam Interactions with Materials and Atoms*, vol. 268, no. 3-4, pp. 334–340, 2010.

[51] N. C. Popa, "The (*hkl*) dependence of diffraction-line broadening caused by strain and size for all Laue groups in Rietveld refinement," *Journal of Applied Crystallography*, vol. 31, no. 2, pp. 176–180, 1998.

[52] C. S. Ciobanu, S. L. Iconaru, F. Massuyeau, L. V. Constantin, A. Costescu, and D. Predoi, "Synthesis, structure, and luminescent properties of europium-doped hydroxyapatite nanocrystalline powders," *Journal Nanomaterials*, vol. 2012, Article ID 942801, 9 pages, 2012.

[53] M. Markovic, B. O. Fowler, and M. S. Tung, "Preparation and comprehensive characterization of a calcium hydroxyapatite reference material," *Journal of Research of the National Institute of Standards and Technology*, vol. 109, no. 6, pp. 553–568, 2004.

[54] W. Jastrzbski, M. Sitarz, M. Rokita, and K. Bułat, "Infrared spectroscopy of different phosphates structures," *Spectrochimica Acta A: Molecular and Biomolecular Spectroscopy*, vol. 79, no. 4, pp. 722–727, 2011.

[55] J. C. Elliott, *Structure and Chemistry of the Apatites and Other Calcium, Orthophosphates*, Elsevier Science, Amsterdam, The Netherlands, 1994.

[56] R. Z. LeGeros, *Calcium Phosphates in Oral Biology and Medicine. Monographs in Oral Sciences*, Karger, Basel, Switzerland, 1991.

[57] C. S. Ciobanu, E. Andronescu, B. S. Vasile, C. M. Valsangiacom, R. V. Ghita, and D. Predoi, "Looking for new synthesis of hydroxyapatite doped with europium," *Optoelectronics and Advanced Materials, Rapid Communications*, vol. 4, no. 10, pp. 1515–1519, 2010.

[58] X. Bai, K. More, C. M. Rouleau, and A. Rabiei, "Functionally graded hydroxyapatite coatings doped with antibacterial components," *Acta Biomaterialia*, vol. 6, no. 6, pp. 2264–2273, 2010.

[59] K. Nakamoto, *Infrared and Raman Spectra of Inorganic and Coordination Compounds*, Wiley, New York, NY, USA, 1978.

[60] R. Z. LeGeros, G. Bonel, and R. Legros, "Types of "H_2O" in human enamel and in precipitated apatites," *Calcified Tissue Research*, vol. 26, no. 1, pp. 111–118, 1978.

[61] M. Eriksson, Y. Liu, J. Hu, L. Gao, M. Nygren, and Z. Shen, "Transparent hydroxyapatite ceramics with nanograin structure prepared by high pressure spark plasma sintering at the minimized sintering temperature," *Journal of the European Ceramic Society*, vol. 31, no. 9, pp. 1533–1540, 2011.

[62] I. Cacciotti and A. Bianco, "High thermally stable Mg-substituted tricalcium phosphate via precipitation," *Ceramics International*, vol. 37, no. 1, pp. 127–137, 2011.

[63] E. I. Get'man, S. N. Loboda, T. V. Tkachenko, N. V. Yablochkova, and K. A. Chebyshev, "Isomorphous substitution of samarium and gadolinium for calcium in hydroxyapatite structure," *Russian Journal of Inorganic Chemistry*, vol. 55, no. 3, pp. 333–338, 2010.

[64] M. P. Casaletto, S. Kaciulis, G. Mattogno, A. Mezzi, L. Ambrosio, and F. Branda, "XPS characterization of biocompatible hydroxyapatite-polymer coatings," *Surface and Interface Analysis*, vol. 34, no. 1, pp. 45–49, 2002.

[65] C. S. Ciobanu, S. L. Iconaru, M. C. Chifriuc, A. Costescu, P. le Coustumer, and D. Predoi, "Synthesis and antimicrobial activity of silver-doped hydroxyapatite nanoparticles," *BioMed Research International*, vol. 2013, Article ID 916218, 10 pages, 2013.

[66] Y. Kim, H. Schleg, K. Kim, J. T. S. Irvine, and J. H. Kim, "X-ray photoelectron spectroscopy of Sm-doped layered perovskite forintermediate temperature-operating solid oxide fuel cell," *Applied Surface Science*, vol. 288, pp. 695–701, 2014.

[67] C. S. Ciobanu, F. Massuyeau, L. V. Constantin, and D. Predoi, "Structural and physical properties of antibacterial Ag-doped nano-hydroxyapatite synthesized at 100°C," *Nanoscale Research Letters*, vol. 6, article 613, 2011.

[68] O. Dubok, O. Shynkaruk, and E. Buzaneva, "Lanthanides oxides usage to increase radiopaque of bioactive ceramics," *Functional Materials*, vol. 20, no. 2, pp. 172–178, 2013.

[69] I. G. Sia, E. F. Berbari, and A. W. Karchmer, "Prosthetic joint infections," *Infectious Disease Clinics of North America*, vol. 19, no. 4, pp. 885–914, 2005.

[70] P. Hsieh, M. S. Lee, K. Hsu, Y. Chang, H. Shin, and S. W. Ueng, "Gram-negative prosthetic joint infections: risk factors and outcome of treatment," *Clinical Infectious Diseases*, vol. 49, no. 7, pp. 1036–1043, 2009.

[71] I. Uçkay and L. Bernard, "Gram-negative versus gram-positive prosthetic joint infections," *Clinical Infectious Diseases*, vol. 50, no. 5, p. 795, 2010.

[72] B. Zmistowski, C. J. Fedorka, E. Sheehan, G. Deirmengian, M. S. Austin, and J. Parvizi, "Prosthetic joint infection caused by gram-negative organisms," *Journal of Arthroplasty*, vol. 26, no. 6, pp. 104–108, 2011.